

Reactive Monte Carlo Simulations for Charge Regulation

Amin Bakhshandeh,[†] Derek Frydel,[‡] and Yan Levin^{*,†}

[†]*Instituto de Física, Universidade Federal do Rio Grande do Sul, Caixa Postal 15051, CEP 91501-970, Porto Alegre, RS, Brazil.*

[‡]*Department of Chemistry, Federico Santa Maria Technical University, Campus San Joaquín, 7820275, Santiago, Chile*

E-mail: levin@if.ufrgs.br

Abstract

We present a reactive Monte Carlo simulation method to study acid-base equilibrium that controls charge regulation in colloidal systems. The simulations use a semi-grand canonical ensemble in which colloidal suspension is in contact with a reservoir of salt and strong acid. The surface reactions are controlled by the equilibrium constants, which correspond to either the internal partition function of a protonated acid surface group or a group with a specifically adsorbed cation. The interior of colloidal particles is modeled as a low dielectric medium, different from the surrounding water. The effective colloidal charge is calculated for different number of surface acidic groups, pH, salt concentrations, and types of electrolyte. The results are compared with the experimental measurements of the effective colloidal charge obtained using potentiometric titration. Excellent agreement is found between simulations and experiments.

The interplay between electrostatic interactions¹⁻²¹ and acid-base equilibrium is of paramount importance in Chemistry and Biology.²²⁻²⁷ It often defines the boundary between life and

death. The protein functionality can change due to modification of surrounding pH, affecting enzymatic activity and the resulting metabolic processes.²⁸ The transport of ions through the cellular membranes²⁹ is strongly affected by pH. The same is true for the binding of heavy metals to bacterial membrane.^{30–32} In biological systems pH, which depends on the activity of proton inside the solution, can be significantly modified by the presence of electrolyte, which at physiological concentration is around 150 mM,^{33,34} affecting the solubility and stability of proteins.^{27,34–40,40–45} In colloidal science both pH and electrolyte concentration regulate colloidal charge and interaction between the particles.^{13,16,46,47}

In the present paper we will present a Monte Carlo method which allows us to efficiently explore the effective charge of colloidal particles inside an electrolyte solution of a given pH. Differently from constant pH simulations,^{38,39} we treat all ions, including hydronium, explicitly in the grand-canonical ensemble. The advantage of this approach is that it automatically enforces uniform electrochemical potential of all ion inside the simulation cell.^{48–52} The colloidal particles are modeled as low dielectric spheres with active surface groups which can become protonated or deprotonated, depending on pH and electrolyte concentration of the suspension. We will also show how the simulation method can be easily adopted to account for the specific ionic adsorption responsible the Hofmeister effect.

Our system consists of a colloidal particle of radius a confined at the center of a spherical Wigner-Seitz (WS) cell of radius R , determined by the volume fraction of colloidal particles in the experimental system. The cell is connected to a reservoir containing strong monovalent salt and acid, at concentrations c_s and c_a , respectively, see Fig. 1. Both salt and acid are assumed to be fully dissociated. All ions have charge $\pm q$, where q is the proton charge. Polystyrene latex particles have a low dielectric core of $\epsilon_c \approx 2.5$, while the dielectric constant of the surrounding water is $\epsilon_w \approx 80$. To stabilize suspension against precipitation, acidic surface groups are often synthesized at the surface of colloidal particles. The surface groups are molecules of weak acid, which partially dissociate, according to the reaction $\text{HA} \rightleftharpoons \text{H}^+ + \text{A}^-$, with a corresponding surface dissociation constant K_a . The protonated and de-

protonated groups, HA and A^- , are also referred as the titration sites, on account of their ability to interact with H^+ . Since the electronic charge of the surface groups does not like the low dielectric environment of the colloidal core, it will shift into the aqueous phase. In our model this will be represented by small spherical sites of radius $r_0 = 2\text{\AA}$ on the surface of colloidal particle. Each titration site in its deprotonated state carries a charge $-q$, and in the protonated state charge 0, see Fig. 1. The cell also contains strong electrolyte $KCl \rightarrow K^+ + Cl^-$ and strong acid $HCl \rightarrow H^+ + Cl^-$, both of which are fully dissociated. Note that inside solution, proton H^+ , associates with a water molecule forming a hydronium ion, H_3O^+ . For simplicity, we will assume that all the ions have the same hydrated radius of 3.3\AA .⁵³

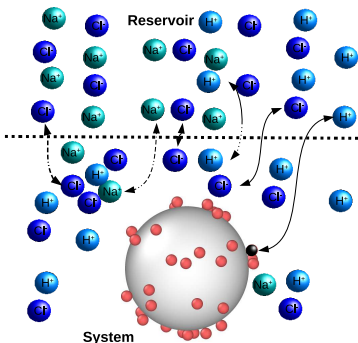


Figure 1: Schematic representation of reactive MC moves. The deprotonated acidic groups A^- on the colloidal surface are represented by the red spheres and protonated HA groups are represented by the black spheres. The protonation of a titration site, $A^- + H^+ \rightarrow HA$, changes its charge from $-1q \rightarrow 0$, at the same time Cl^- is added to the cell with grand canonical probability, to preserve the overall charge neutrality. Deprotonation reaction, $HA \rightarrow A^- + H^+$, results in the change $0 \rightarrow -1q$ of the titration site, and a simultaneous removal of Cl^- from the simulation cell.

The dielectric contrast between the colloidal core and the surrounding water results in induced surface charge density at the interface. The surface charge distribution depends on the location of ions inside the suspension. Therefore, the interaction between any two ions will not be given simply by the Coulomb potential, but will also depend on their distance from the colloidal surface. The Green function for the effective interaction between two ions is very accurately approximated by⁵⁴⁻⁵⁶

$$G(\mathbf{r}, \mathbf{r}') = \frac{1}{\epsilon_w |\mathbf{r} - \mathbf{r}'|} + \frac{\gamma a}{\epsilon_w r' |\mathbf{r} - \frac{a^2}{r'^2} \mathbf{r}'|} + \gamma \psi_c(\mathbf{r}, \mathbf{r}'), \quad (1)$$

with

$$\psi_c(\mathbf{r}, \mathbf{r}') = \frac{1}{\epsilon_w a} \ln \left[\frac{rr' - \mathbf{r} \cdot \mathbf{r}'}{a^2 - \mathbf{r} \cdot \mathbf{r}' + \sqrt{a^4 - 2a^2(\mathbf{r} \cdot \mathbf{r}') + r^2 r'^2}} \right], \quad (2)$$

where $\gamma = (\epsilon_w - \epsilon_c) / (\epsilon_w + \epsilon_c)$. The first term of Eq. 1 is due to the direct Coulomb potential produced by an ion located at position \mathbf{r}' from the center of colloidal particle, while other two terms result from the induced surface charge.^{57,58} Note that the Green function is invariant under the exchange of the source and the observation points $\mathbf{r} \leftrightarrow \mathbf{r}'$. Eq. 1 is exact in the limit $\epsilon_c/\epsilon_w \rightarrow 0$, $\gamma = 1$. Furthermore, it was shown that it remains very accurate for $\epsilon_c/\epsilon_w \ll 1$,⁵⁵ which is appropriate for the present system with $\epsilon_c/\epsilon_w = 2.5/80$.

The internal energy of the system is:

$$U = \sum_{i=1}^N \left[\frac{q^2 \gamma a}{2\epsilon_w (r_i^2 - a^2)} + \frac{q\gamma \psi_{self}(\mathbf{r}_i)}{2} \right] + \sum_{i=1}^{N-1} \sum_{j=i+1}^N q_i q_j G(\mathbf{r}_i, \mathbf{r}_j), \quad (3)$$

where N is the total number of particles inside the cell, including the charged surface sites. The term in the square brackets is due to the self-interaction of an ion with its own induced surface charge, where ψ_{self} is given by

$$\psi_{self}(\mathbf{r}_i) = \frac{q}{\epsilon_w a} \ln \left(1 - \frac{a^2}{r_i^2} \right). \quad (4)$$

Simulation —The simulations are performed in the grand canonical ensemble, in which the system is in contact with an infinite reservoir of strong acid and salt. Since the Wigner-Seitz cell represents an infinite colloidal suspension at finite concentration, we must think of it as being separated from the reservoir by a semipermeable membrane which allows for a free passage of ions, but not of colloidal particles. The diffusion of ions will result in an

electric field across the membrane, establishing a potential difference between the system and the reservoir. This is known as the Donnan potential, φ_D . When an ion moves from the reservoir into the system it will, therefore, gain additional energy $q_i\varphi_D$.

Our reactive Monte Carlo involves two types of movements. The standard grand canonical insertion/deletion of ions between the reservoir and the simulation cell; and protonation and deprotonation moves for the surface sites. The grand canonical acceptance probabilities for insertion or deletion of a particle of type i are given by $ACC = \min(1, \phi_{add/rem})$ where $\phi_{add/rem}$ is

$$\begin{aligned}\phi_{add} &= \frac{Vc_i}{N_i + 1} \exp[-\beta(\Delta E_{ele} - \mu_{ex} + q_i\varphi_D)], \\ \phi_{rem} &= \frac{N_i}{Vc_i} \exp[-\beta(\Delta E_{ele} + \mu_{ex} - q_i\varphi_D)].\end{aligned}\tag{5}$$

Here ΔE_{ele} is the change in electrostatic energy upon insertion or deletion of an ion, μ_{ex} is the excess chemical potential of ions in the reservoir, and V is the free volume accessible to the ions. Note that since all ions are assumed to have the same radius, the excess chemical potential of all ions is the same. The Donnan potential φ_D has to be adjusted each few MC steps to keep charge neutrality inside the system.⁵⁹ This makes simulations slow. A simple solution to this problem is to perform insertion or deletion of cations-anion pairs, so that the charge neutrality of the cell is always preserved. For example, the probability of insertion/deletion of KCl pair is the product $\phi_{add/rem}^{K^+}\phi_{add/rem}^{Cl^-}$, so that the Donnan potential cancels out. The excess chemical potential μ_{ex} of ions has two contributions: the electrostatic and the excluded volume. Given the concentration of acid and salt in the reservoir, the electrostatic contribution to μ_{ex} can be calculated very accurately using the mean-spherical approximation (MSA) $\beta\mu_{MSA} = \frac{\lambda_B(\sqrt{1+2\kappa d}-\kappa d-1)}{d^2\kappa}$,⁶⁰⁻⁶⁵ where d is the diameter of the ions, $c_t = c_s + c_a$ is the total concentration of salt and acid, $\lambda_B = q^2/\epsilon_w k_B T$ is the Bjerrum length, and $\kappa = \sqrt{8\pi\lambda_B c_t}$ is the inverse Debye length. The excluded volume contribution to the excess chemical potential is well approximated by the Carnahan-Starling

theory $\beta\mu_{CS} = \frac{8\eta - 9\eta^2 + 3\eta^3}{(1-\eta)^3}$,⁶⁶⁻⁶⁹ where the volume fraction is $\eta = \frac{\pi d^3}{3}c_t$. The total excess chemical potential of an ion is then $\mu_{ex} = \mu_{CS} + \mu_{MSA}$. To test the accuracy of these expression, we performed grand canonical MC (GCMC) simulations⁷⁰ in which initially empty simulation cell is connected with a salt and acid reservoir. The electrostatic interactions are calculated using Ewald summation. The concentration of acid inside the reservoir is fixed at $c_a = 1\text{mM}$, and of salt is varied from 0 to 300mM. The insertions and deletions of ions in the GCMC simulations are performed using the excess chemical potential presented above. If μ_{ex} is accurate for both electrostatic and excluded volume interactions, the concentration of ions in the simulation cell will equilibrate to the same values fixed in the reservoir. This is precisely what is observed in simulations. see Fig. 2. demonstrating the accuracy of μ_{ex} .

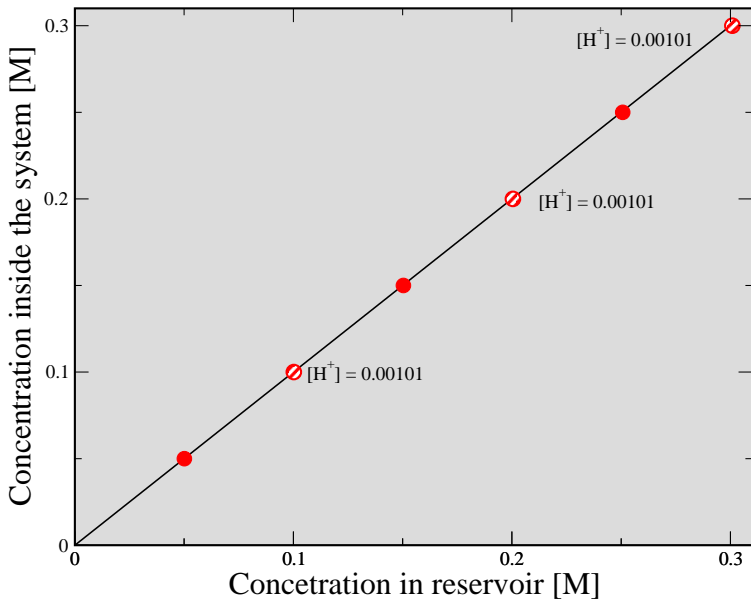


Figure 2: Salt concentration inside the system as a function of the reservoir concentration. The reservoir also contains strong acid at concentration $c_a = 0.001\text{M}$. The straight line indicates the theoretical expectation that the concentrations of ions inside the system should be exactly the same as the concentration of ions in the reservoir. The concentration of hydronium ion inside the system is indicated next to the symbols. The excellent agreement between concentrations inside the system and in the reservoir indicates accuracy of our expression for μ_{ex} .

To obtain the MC weights for protonation/deprotonation moves, we first consider the free energy change for a reaction of a hydronium ion with an isolated weak acid group A^- ,

$\text{H}_3\text{O}^+ + \text{A}^- \rightleftharpoons \text{HA} + \text{H}_2\text{O}$. We can think of this process as a removal of a hydronium ion from the reservoir, followed by a reaction with a A^- group. The internal partition function of the HA molecule is $K_{eq}/\Lambda_{\text{H}^+}^3$, where K_{eq} is the equilibrium constant and Λ_{H^+} is the hydronium's de Broglie thermal wavelength. The free energy change of the system+reservoir resulting from the removal of a hydronium ion from the reservoir and bringing it into vicinity of A^- , where it will undergo a proton transfer reaction, is then $\beta\Delta F_p = -\ln(K_{eq}/\Lambda_{\text{H}^+}^3) - \mu_{\text{H}^+}$, where $\beta\mu_{\text{H}^+} = \ln(c_{\text{H}^+}\Lambda_{\text{H}^+}^3) + \beta\mu_{ex}$ is the total chemical potential of a hydronium ion inside the reservoir. For the deprotonation reaction the free energy change is $\Delta F_d = -\Delta F_p$. The acceptance probabilities for protonation and deprotonation moves are, therefore,

$$\begin{aligned}\phi_p &= \exp[-\beta(\Delta E_{ele} + \Delta F_p + q\varphi_D)], \\ \phi_d &= \exp[-\beta(\Delta E_{ele} + \Delta F_d - q\varphi_D)],\end{aligned}\tag{6}$$

respectively. These simplify to

$$\begin{aligned}\phi_p &= c_{\text{H}^+}K_{eq} \exp[-\beta(\Delta E_{ele} - \mu_{ex} + q\varphi_D)], \\ \phi_d &= \frac{1}{c_{\text{H}^+}K_{eq}} \exp[-\beta(\Delta E_{ele} + \mu_{ex} - q\varphi_D)].\end{aligned}\tag{7}$$

A Monte Carlo "reaction" move consists of selecting a random titration site, followed by an attempt to change its "state" from protonated to deprotonated and vice versa. Note that the acceptance probabilities depend on the Donnan potential, which is *a priori*, unknown. We can overcome this difficulty by again combining the protonation attempt with an insertion of Cl^- . The probability of acceptance of a protonation- Cl^- -insertion move is then $\min\{1, \phi_p\phi_{add}\}$. In the product, the Donnan potential once again cancels out. Similarly a deprotonation move is combined with a removal of Cl^- , so that the probability is

$\min\{1, \phi_d \phi_{rem}\}$. The final acceptance probabilities for the pair moves are:

$$\begin{aligned}\phi_{d+rem} &= \frac{N_{\text{Cl}^-}}{c_{\text{H}^+} K_{eq} V c_{\text{Cl}^-}} \exp[-\beta(\Delta E_{ele} + 2\mu_{ex})], \\ \phi_{p+add} &= \frac{c_{\text{H}^+} K_{eq} V c_{\text{Cl}^-}}{(N_{\text{Cl}^-} + 1)} \exp[-\beta(\Delta E_{ele} - 2\mu_{ex})]\end{aligned}\tag{8}$$

where N_{Cl^-} is the number of Cl^- ions inside the cell. In Fig. 1 we have schematically shown these movements.

We now apply the simulation method discussed above to study the effective charge of carboxy latex particles,⁷¹ the surface sites of which undergo reaction $-\text{COOH} \rightleftharpoons \text{COO}^- + \text{H}^+$. The simulated system consists of a spherical cell of radius $R = 120\text{\AA}$, with a spherical colloidal particle at the center, represented by a hard-sphere of radius $a = 60\text{\AA}$, with surface titration sites of $r_0 = 2\text{\AA}$, see Fig. 1.

The mobile ions correspond to the dissociation of KCl and HCl. We are interested in obtaining the effective charge of a colloidal particle as a function of pH and salt concentration in the reservoir. Recall that $\text{pH} = -\log[a_{\text{H}^+}]$, where $a_{\text{H}^+} = c_{\text{H}^+} \exp[\beta\mu_{ex}(c_t)]$ is the activity of hydronium ions. We consider two different carboxyl latex colloidal particles, the effective charge of which has been obtained experimentally using potentiometric titration.⁷¹ It is important to remember that the surface association constant K_{eq} is different from the bulk association constant for the same acid.⁷²⁻⁷⁷ This difference may be attributed to the distinct symmetry of the electronic wave function of chemical group when it is on the surface of colloidal particle and when it is in the bulk. Our strategy, then, is to adjust K_{eq} to fit the experimental titration curve for colloidal particles with the bare surface charge density $\sigma_T = 78 \text{ mC/m}^2$ – determined by the total number of surface carboxyl groups – inside the electrolyte solution of $c_{\text{KCl}} = 10 \text{ mM}$. We will then use the *same* K_{eq} to calculate the theoretical titration curves for other salt concentrations and different colloidal bare charge. Recalling that acid dissociation constant is $K_a = 1/K_{eq}$, we obtain an excellent fit of the experimental titration curve using $\text{p}K_a = -\log[K_a] = \log[K_{eq}] = 5.02$, see Fig. 3(a). We

next use the same value of pK_a to calculate the titration curve for a particle of the same bare surface charge inside an electrolyte solution of 300mM, observing a good agreement with the experimentally obtained titration curves, Fig. 3(b). Finally, we calculate the titration curves for colloidal particles of surface charge $\sigma_T = 98 \text{ mC/m}^2$, in solutions of 10mM and 300mM electrolyte, using the *same* surface equilibrium constant as before. Once again a very good agreement is found between simulations and experiments, see Fig. 3 panels (c) and (d).

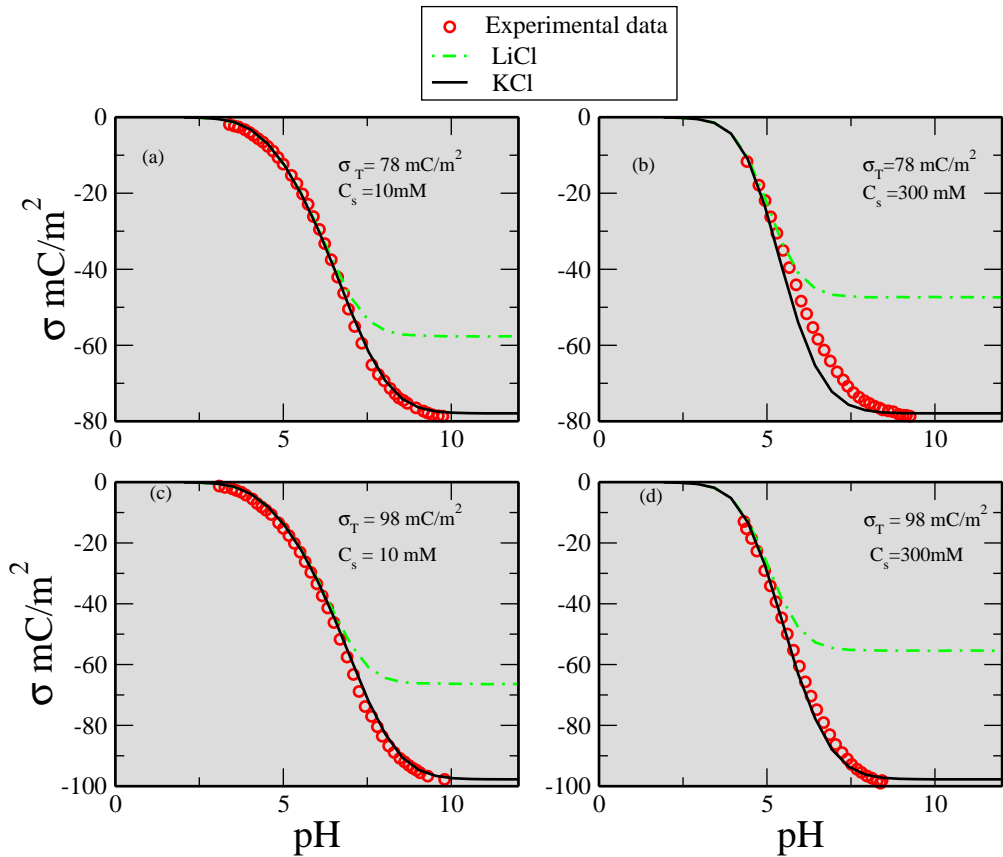


Figure 3: Effective charge obtained using the reactive MC simulations (curves) compared with the experimental data (symbols). The solid black curve is the effective charge in the presence of KCl and dashed green curve in the presence of LiCl. The bare surface charge densities of colloidal particles are 78 mC/m^2 panels (a) and (b); and 98 mC/m^2 panels (c) and (d). Electrolyte concentration is indicated in each panel. The surface equilibrium constant, $pK_a = 5.02$ is obtained by fitting the experimental data in the panel (a). The *same* equilibrium constant is then used to calculate the effective charges for other salt concentrations and colloidal bare charge: panels (b), (c) and (d). A very good agreement is observed between theory and experiment.⁷¹

We next show how the specific ion adsorption can also be easily included within the

simulation formalism introduced above. It is known that Li^+ specifically associate with COO^- .^{78,79} We are, therefore, interested to explore the effect of replacing KCl with LiCl salt. The specific association of Li^+ with COO^- is a consequence of the law of matching water affinities (LMWA),⁸⁰ which suggests that both lithium and carboxylate can lose part of their hydration sheath resulting in strong electrostatic interaction between the two ions. LiCOO can exist in two states - contact ion pair (CIP) and solvent separated ion pair (SIP).⁸¹⁻⁸⁶ Based on LMWA we will take the distance of closest approach between lithium and carboxylate contact pair to be $d = 2.9\text{\AA}$, corresponding to the Latimer diameter of Li^+ ion.^{87,88} The surface lithium-carboxylate association constant for CIP, K_{Li} , can then be calculated using Bjerrum theory:⁶²

$$K_{\text{Li}} = 2\pi \int_0^{\pi - \cos^{-1}\left(\frac{r_0 - d/2}{d}\right)} \int_d^{\lambda_B/2} e^{-\beta u(r,\theta)} \sin \theta r^2 dr d\theta \quad (9)$$

where $u(r)$ is

$$u(r) = \frac{\lambda_B}{r} + \frac{\lambda_B}{\sqrt{4r_0^2 + r^2 + 4r_0r \cos \theta}} - \frac{\lambda_B}{4(r_0 + r \cos \theta)}, \quad (10)$$

The first term in the exponential is the direct Coulomb interaction, the second term is the interaction of lithium ion with the image of carboxylate inside the colloidal core, and the last term is the interaction of lithium with its own image. Since the resulting CIP is much smaller than colloidal radius, we neglect the curvature of colloidal surface in calculation of K_{Li} . Eq. 10 can be evaluated numerically yielding $K_{\text{Li}} = 922.331 \text{\AA}^3$. The specific association of Li^+ is then treated in the same way as H^+ , using the acceptance probabilities Eq.(8), but with $K_{eq} \rightarrow K_{\text{Li}}$. This way we account for CIP configuration, the SIP states appear naturally in the simulation when hydrated Li^+ ions come near hydrated COO^- groups. In Fig. 3 (dashed green curve) we show the effect of replacing K^+ with Li^+ on the effective colloidal charge. Note the saturation of colloidal charge at large pH, resulting from the association of Li^+ ions with the carboxylate groups. Specific adsorption of Li^+ , also affects the protonation of carboxylate. In Fig. 4 we show the fraction of protonated groups in suspensions with KCl

or LiCl salts.

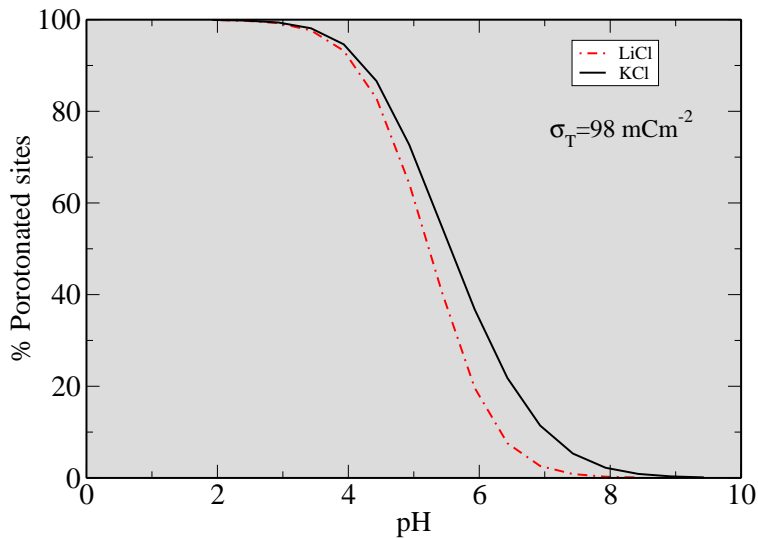


Figure 4: The fraction of protonated groups in the presence of 300mM of either KCl or LiCl salts. Specific adsorption of Li^+ to carboxylate groups results in stronger deprotonation, in particular at large pH.

We have presented a simulation method which allows us to very accurately calculate the titration curves for suspensions of colloidal particles. The results were compared with the experimental measurements of the effective colloidal charge obtained using potentiometric titration. Excellent agreement was found between simulations and experiments. We have also shown how the specific ion interaction, responsible for the Hofmeister effect can be easily included in the simulation method. The approach presented in this Letter can be also applied to other scientifically and technologically important systems, such as proteins, polyelectrolyte gels, polyampholytes, etc.

This work was partially supported by the CNPq, CAPES, National Institute of Science and Technology Complex Fluids INCT-FCx. The authors are grateful to the Instituto de Física e Matemática, UFPel for the use of computer resources. D.F. acknowledges financial support from FONDECYT through grant number 1201192.

References

- (1) Prusty, D.; Nap, R. J.; Szleifer, I.; Olvera de la Cruz, M. Charge regulation mechanism in end-tethered weak polyampholytes. *Soft Matter* **2020**, *16*, 8832–8847.
- (2) Leung, C.-Y.; Palmer, L. C.; Kewalramani, S.; Qiao, B.; Stupp, S. I.; Olvera de la Cruz, M.; Bedzyk, M. J. Crystalline polymorphism induced by charge regulation in ionic membranes. *Proceedings of the National Academy of Sciences* **2013**, *110*, 16309–16314.
- (3) Javidpour, L.; Božič, A.; Naji, A.; Podgornik, R. Electrostatic interaction between SARS-CoV-2 virus and charged electret fibre. *Soft Matter* **2021**, –.
- (4) Javidpour, L.; Božič, A. L.; Podgornik, R.; Naji, A. Role of metallic core for the stability of virus-like particles in strongly coupled electrostatics. *Scientific reports* **2019**, *9*, 1–13.
- (5) Fink, L.; Allolio, C.; Feitelson, J.; Tamburu, C.; Harries, D.; Raviv, U. Bridges of Calcium Bicarbonate Tightly Couple Dipolar Lipid Membranes. *Langmuir* **2020**, *36*, 10715–10724, PMID: 32787004.
- (6) Kubincová, A.; Hünenberger, P. H.; Krishnan, M. Interfacial solvation can explain attraction between like-charged objects in aqueous solution. *J. Chem. Phys.* **2020**, *152*, 104713.
- (7) Krishnan, M. A simple model for electrical charge in globular macromolecules and linear polyelectrolytes in solution. *J. Chem. Phys.* **2017**, *146*, 205101.
- (8) Krishnan, M. Electrostatic free energy for a confined nanoscale object in a fluid. *J. Chem. Phys.* **2013**, *138*, 114906.
- (9) Behjatian, A.; Bessalova, M.; Karedla, N.; Krishnan, M. Electroviscous effect for a confined nanosphere in solution. *Phys. Rev. E* **2020**, *102*, 042607.

- (10) Ma, B.; Olvera de la Cruz, M. A Perspective on the Design of Ion-Containing Polymers for Polymer Electrolyte Applications. *The Journal of Physical Chemistry B* **0**, *0*, null, PMID: 33635658.
- (11) Gao, C.; Kewalramani, S.; Valencia, D. M.; Li, H.; McCourt, J. M.; Olvera de la Cruz, M.; Bedzyk, M. J. Electrostatic shape control of a charged molecular membrane from ribbon to scroll. *Proceedings of the National Academy of Sciences* **2019**, *116*, 22030–22036.
- (12) Avni, Y.; Podgornik, R.; Andelman, D. Critical behavior of charge-regulated macroions. *The Journal of Chemical Physics* **2020**, *153*, 024901.
- (13) Avni, Y.; Andelman, D.; Podgornik, R. Charge regulation with fixed and mobile charged macromolecules. *Curr Opin Electrochem* **2019**, *13*, 70–77.
- (14) Adar, R. M.; Andelman, D.; Diamant, H. Electrostatics of patchy surfaces. *Advances in Colloid and Interface Science* **2017**, *247*, 198–207, Dominique Langevin Festschrift: Four Decades Opening Gates in Colloid and Interface Science.
- (15) Shen, H.; Frey, D. D. Effect of charge regulation on steric mass-action equilibrium for the ion-exchange adsorption of proteins. *J. Chromatogr. A* **2005**, *1079*, 92 – 104.
- (16) Tsao, H. K. Electrostatic interaction of an assemblage of charges with a charged surface: the charge-regulation effect. *Langmuir* **2000**, *16*, 7200–7209.
- (17) Löwen, H.; Esztermann, A.; Wysocki, A.; Allahyarov, E.; Messina, R.; Jusufi, A.; Hoffmann, N.; Gottwald, D.; Kahl, G.; Konieczny, M.; Likos, C. N. Charged colloids and polyelectrolytes: from statics to electrokinetics. *Journal of Physics: Conference Series* **2005**, *11*, 207–222.
- (18) Messina, R.; Holm, C.; Kremer, K. Like-charge colloid–polyelectrolyte complexation. *The Journal of Chemical Physics* **2002**, *117*, 2947–2960.

- (19) Messina, R.; Holm, C.; Kremer, K. Charge inversion in colloidal systems. *Computer Physics Communications* **2002**, *147*, 282–285, Proceedings of the Europhysics Conference on Computational Physics Computational Modeling and Simulation of Complex Systems.
- (20) Borkovec, M.; Jönsson, B.; Koper, G. J. M. In *Surface and Colloid Science*; Matijević, E., Ed.; Springer US: Boston, MA, 2001; pp 99–339.
- (21) Narambuena, C. F.; Blanco, P. M.; Rodriguez, A.; Rodriguez, D. E.; Madurga, S.; Garcés, J. L.; Mas, F. Non-monotonic behavior of weak-polyelectrolytes adsorption on a cationic surface: A Monte Carlo simulation study. *Polymer* **2021**, *212*, 123170.
- (22) Worms, I.; Simon, D. F.; Hassler, C.; Wilkinson, K. Bioavailability of trace metals to aquatic microorganisms: importance of chemical, biological and physical processes on biouptake. *Biochimie* **2006**, *88*, 1721–1731.
- (23) Booth, I. R. Regulation of cytoplasmic pH in bacteria. *Microbiological reviews* **1985**, *49*, 359.
- (24) Antelo, J.; Avena, M.; Fiol, S.; López, R.; Arce, F. Effects of pH and ionic strength on the adsorption of phosphate and arsenate at the goethite–water interface. *Journal of colloid and interface science* **2005**, *285*, 476–486.
- (25) Brigante, M.; Avena, M. Biotemplated synthesis of mesoporous silica for doxycycline removal. Effect of pH, temperature, ionic strength and Ca²⁺ concentration on the adsorption behaviour. *Microporous and Mesoporous Materials* **2016**, *225*, 534–542.
- (26) Hammes, F.; Verstraete, W. Key roles of pH and calcium metabolism in microbial carbonate precipitation. *Reviews in environmental science and biotechnology* **2002**, *1*, 3–7.

- (27) Teixeira, A. A. R.; Lund, M.; Barroso da Silva, F. L. Fast proton titration scheme for multiscale modeling of protein solutions. *Journal of chemical theory and computation* **2010**, *6*, 3259–3266.
- (28) Kurkdjian, A.; Guern, J. Intracellular pH: Measurement and Importance in Cell Activity. *Annual Review of Plant Physiology and Plant Molecular Biology* **1989**, *40*, 271–303.
- (29) Accardi, A.; Miller, C. Secondary active transport mediated by a prokaryotic homologue of ClC Cl-channels. *Nature* **2004**, *427*, 803–807.
- (30) Beveridge, T. J. Role of cellular design in bacterial metal accumulation and mineralization. *Annual review of microbiology* **1989**, *43*, 147–171.
- (31) van der Wal, A.; Norde, W.; Zehnder, A. J.; Lyklema, J. Determination of the total charge in the cell walls of Gram-positive bacteria. *Colloids and surfaces B: Biointerfaces* **1997**, *9*, 81–100.
- (32) Heinrich, H. T.; Bremer, P. J.; Daughney, C. J.; McQuillan, A. J. Acid- Base Titrations of Functional Groups on the Surface of the Thermophilic Bacterium *Anoxybacillus flavithermus*: Comparing a Chemical Equilibrium Model with ATR-IR Spectroscopic Data. *Langmuir* **2007**, *23*, 2731–2740.
- (33) Pressman, B. C. Induced active transport of ions in mitochondria. *Proceedings of the National Academy of Sciences of the United States of America* **1965**, *53*, 1076.
- (34) Lund, M.; Jönsson, B. Charge regulation in biomolecular solution. *Q. Rev. Biophys.* **2013**, *46*, 265–281.
- (35) Lunkad, R.; Murmiliuk, A.; Hebbeker, P.; Boublík, M.; Tošner, Z.; Štěpánek, M.; Košovan, P. Quantitative prediction of charge regulation in oligopeptides. *Mol. Syst. Des. Eng.* **2021**, *6*, 122–131.

- (36) Lunkad, R.; Murmiliuk, A.; Tošner, Z.; Štěpánek, M.; Košovan, P. Role of pKA in Charge Regulation and Conformation of Various Peptide Sequences. *Polymers* **2021**, *13*, 214.
- (37) Perutz, M. Electrostatic effects in proteins. *Science* **1978**, *201*, 1187–1191.
- (38) Svensson, B.; Jönsson, B.; Woodward, C. Electrostatic contributions to the binding of Ca²⁺ in calbindin mutants: a Monte Carlo study. *Biophysical chemistry* **1990**, *38*, 179–183.
- (39) Woodward, C.; Svensson, B. R. Potentials of mean force in charged systems: Application to Superoxide Dismutase. *The Journal of Physical Chemistry* **1991**, *95*, 7471–7477.
- (40) Lund, M.; Jönsson, B. On the charge regulation of proteins. *Biochemistry* **2005**, *44*, 5722–5727.
- (41) Dickinson, E.; Leser, M. E. *Food colloids: self-assembly and material science*; Royal Society of chemistry, 2007.
- (42) da Silva, F. L. B.; Jönsson, B. Polyelectrolyte–protein complexation driven by charge regulation. *Soft Matter* **2009**, *5*, 2862–2868.
- (43) Szuttor, K.; Weik, F.; Grad, J.-N.; Holm, C. Modeling the current modulation of bundled DNA structures in nanopores. *The Journal of Chemical Physics* **2021**, *154*, 054901.
- (44) Behrens, S. H.; Grier, D. G. The charge of glass and silica surfaces. *The Journal of Chemical Physics* **2001**, *115*, 6716–6721.
- (45) Lund, M.; Åkesson, T.; Jönsson, B. Enhanced Protein Adsorption Due to Charge Regulation. *Langmuir* **2005**, *21*, 8385–8388.
- (46) Andelman, D. Introduction to electrostatics in soft and biological matter. *Soft condensed matter physics in molecular and cell biology* **2006**, *6*.

- (47) Podgornik, R. General theory of charge regulation and surface differential capacitance. *J. Chem. Phys.* **2018**, *149*, 104701.
- (48) Madurga, S.; Rey-Castro, C.; Pastor, I.; Vilaseca, E.; David, C.; Garcés, J. L.; Puy, J.; Mas, F. A semi-grand canonical Monte Carlo simulation model for ion binding to ionizable surfaces: Proton binding of carboxylated latex particles as a case study. *The Journal of chemical physics* **2011**, *135*, 184103.
- (49) Nishio, T. Monte Carlo studies on potentiometric titration of (carboxymethyl) cellulose. *Biophysical chemistry* **1996**, *57*, 261–267.
- (50) Nishio, T. Monte Carlo simulations on potentiometric titration of cylindrical polyelectrolytes: Introduction of a method and its application to model systems without added salt. *Biophysical chemistry* **1994**, *49*, 201–214.
- (51) Johnson, J. K.; Panagiotopoulos, A. Z.; Gubbins, K. E. Reactive canonical Monte Carlo: a new simulation technique for reacting or associating fluids. *Molecular Physics* **1994**, *81*, 717–733.
- (52) Valleau, J. P.; Cohen, L. K. Primitive model electrolytes. I. Grand canonical Monte Carlo computations. *The Journal of chemical physics* **1980**, *72*, 5935–5941.
- (53) Nightingale Jr, E. Phenomenological theory of ion solvation. Effective radii of hydrated ions. *The Journal of Physical Chemistry* **1959**, *63*, 1381–1387.
- (54) Bakhshandeh, A.; Dos Santos, A. P.; Levin, Y. Weak and strong coupling theories for polarizable colloids and nanoparticles. *Phys. Rev. Lett.* **2011**, *107*, 107801.
- (55) dos Santos, A. P.; Bakhshandeh, A.; Levin, Y. Effects of the dielectric discontinuity on the counterion distribution in a colloidal suspension. *J. Chem. Phys.* **2011**, *135*, 044124.

- (56) Bakhshandeh, A. Theoretical investigation of a polarizable colloid in the salt medium. *Chem. Phys.* **2018**, *513*, 195–200.
- (57) Norris, W. Charge images in a dielectric sphere. *IEE Proceedings-Science, Measurement and Technology* **1995**, *142*, 142–150.
- (58) Lindell, I. V. Image theory for electrostatic and magnetostatic problems involving a material sphere. *American journal of physics* **1993**, *61*, 39–44.
- (59) Barr, S. A.; Panagiotopoulos, A. Z. Grand-canonical Monte Carlo method for Donnan equilibria. *Phys. Rev. E* **2012**, *86*, 016703.
- (60) Ho/ye, J. S.; Lomba, E. Mean spherical approximation (MSA) for a simple model of electrolytes. I. Theoretical foundations and thermodynamics. *The Journal of chemical physics* **1988**, *88*, 5790–5797.
- (61) Ho, C.-H.; Tsao, H.-K.; Sheng, Y.-J. Interfacial tension of a salty droplet: Monte Carlo study. *The Journal of chemical physics* **2003**, *119*, 2369–2375.
- (62) Levin, Y.; Fisher, M. E. Criticality in the hard-sphere ionic fluid. *Physica A: Statistical Mechanics and its Applications* **1996**, *225*, 164–220.
- (63) Waisman, E.; Lebowitz, J. L. Mean spherical model integral equation for charged hard spheres I. Method of solution. *The Journal of Chemical Physics* **1972**, *56*, 3086–3093.
- (64) Waisman, E.; Lebowitz, J. L. Mean spherical model integral equation for charged hard spheres. II. Results. *The Journal of Chemical Physics* **1972**, *56*, 3093–3099.
- (65) Blum, L. Mean spherical model for asymmetric electrolytes: I. Method of solution. *Molecular Physics* **1975**, *30*, 1529–1535.
- (66) Carnahan, N. F.; Starling, K. E. Equation of state for nonattracting rigid spheres. *The Journal of chemical physics* **1969**, *51*, 635–636.

- (67) Carnahan, N. F.; Starling, K. E. Thermodynamic properties of a rigid-sphere fluid. *The Journal of Chemical Physics* **1970**, *53*, 600–603.
- (68) Adams, D. Chemical potential of hard-sphere fluids by Monte Carlo methods. *Molecular Physics* **1974**, *28*, 1241–1252.
- (69) Maciel, J. A. C. d. S. L.; Abreu, C. R. A.; Tavares, F. W. CHEMICAL POTENTIALS OF HARD-CORE MOLECULES BY A STEPWISE INSERTION METHOD. *Brazilian Journal of Chemical Engineering* **2018**, *35*, 277–288.
- (70) Frenkel, D.; Smit, B. *Understanding molecular simulation: from algorithms to applications*; Elsevier, 2001; Vol. 1.
- (71) Behrens, S. H.; Christl, D. I.; Emmerzael, R.; Schurtenberger, P.; Borkovec, M. Charging and aggregation properties of carboxyl latex particles: Experiments versus DLVO theory. *Langmuir* **2000**, *16*, 2566–2575.
- (72) Buffle, J.; Chalmers, R. A. *Complexation reactions in aquatic systems*; John Wiley and Sons Inc., New York, NY, 1988.
- (73) Cera, E. D. *Thermodynamic Theory of Site-Specific Binding Processes in Biological Macromolecules*; Cambridge University Press, 1995.
- (74) Lluís Garcés, J.; Mas, F.; Puy, J.; Galceran, J.; Salvador, J. Use of activity coefficients for bound and free sites to describe metal–macromolecule complexation. *J. Chem. Soc., Faraday Trans.* **1998**, *94*, 2783–2794.
- (75) Bakhshandeh, A.; Frydel, D.; Diehl, A.; Levin, Y. Charge regulation of colloidal particles: Theory and simulations. *Physical review letters* **2019**, *123*, 208004.
- (76) Bakhshandeh, A.; Frydel, D.; Levin, Y. Charge regulation of colloidal particles in aqueous solutions. *Phys. Chem. Chem. Phys.* **2020**, *22*, 24712–24728.

- (77) Gomez, D. A.; Frydel, D.; Levin, Y. Lattice-gas model of a charge regulated planar surface. *The Journal of Chemical Physics* **2021**, *154*, 074706.
- (78) Uejio, J. S.; Schwartz, C. P.; Duffin, A. M.; Drisdell, W. S.; Cohen, R. C.; Saykally, R. J. Characterization of selective binding of alkali cations with carboxylate by x-ray absorption spectroscopy of liquid microjets. *Proceedings of the National Academy of Sciences* **2008**, *105*, 6809–6812.
- (79) Sthoer, A.; Hladílková, J.; Lund, M.; Tyrode, E. Molecular insight into carboxylic acid–alkali metal cations interactions: Reversed affinities and ion-pair formation revealed by non-linear optics and simulations. *Phys. Chem. Chem. Phys.* **2019**, *21*, 11329–11344.
- (80) Collins, K. D. Why continuum electrostatics theories cannot explain biological structure, polyelectrolytes or ionic strength effects in ion–protein interactions. *Biophysical chemistry* **2012**, *167*, 43–59.
- (81) Iwahara, J.; Esadze, A.; Zandarashvili, L. Physicochemical Properties of Ion Pairs of Biological Macromolecules. *Biomolecules* **2015**, *5*, 2435–2463.
- (82) Winstein, S.; Klinedinst Jr, P. E.; Clippinger, E. Salt Effects and Ion Pairs in Solvolysis and Related Reactions. XXI. 1 Acetolysis, Bromide Exchange and the Special Salt Effect². *Journal of the American Chemical Society* **1961**, *83*, 4986–4989.
- (83) Record Jr, M. T.; Lohman, T. M.; De Haseth, P. Ion effects on ligand-nucleic acid interactions. *Journal of molecular biology* **1976**, *107*, 145–158.
- (84) Lü, J.-M.; Rosokha, S. V.; Lindeman, S. V.; Neretin, I. S.; Kochi, J. K. “Separated” versus “contact” ion-pair structures in solution from their crystalline states: dynamic effects on dinitrobenzenide as a mixed-valence anion. *Journal of the American Chemical Society* **2005**, *127*, 1797–1809.

- (85) Masnovi, J.; Kochi, J. Direct observation of ion-pair dynamics. *Journal of the American Chemical Society* **1985**, *107*, 7880–7893.
- (86) Yabe, T.; Kochi, J. Contact ion pairs. Picosecond dynamics of solvent separation, internal return, and special salt effect. *Journal of the American Chemical Society* **1992**, *114*, 4491–4500.
- (87) Diehl, A.; Dos Santos, A. P.; Levin, Y. Surface tension of an electrolyte–air interface: a Monte Carlo study. *Journal of Physics: Condensed Matter* **2012**, *24*, 284115.
- (88) Latimer, W. M.; Pitzer, K. S.; Slansky, C. M. *Molecular Structure And Statistical Thermodynamics: Selected Papers of Kenneth S Pitzer*; World Scientific, 1993; pp 485–489.